# MODELLING OF THE LABORATORY EXPERIMENTS OF SOLUTE TRANSPORT THROUGH A NATURAL ROCK FRACTURE

Authors Antti Poteri, VTT Processes

Pirkko Hölttä, Laboratory of Radiochemistry, University of Helsinki

Publicity: Free

| Research organisation and address | Customer |
|---|---|
| VTT Processes,<br>P.O. Box 1608<br>FI-02044 VTT, FINLAND | Valtion ydinjätehuoltorahasto<br>Kauppa- ja teollisuusministeriö<br>PL 32<br>00023 VALTIONEUVOSTO |
| **Responsible person**<br>Antti Poteri | **Contact person**<br>Anne Väätäinen (KTM) |
| **Diary code (VTT)**<br>PRO1-105T-03 | **Order reference**<br>15/2004/KYT |
| **Title and reference code for assignment**<br>Kulkeutuminen kallion raoissa, 13KYT-KULKE | **Report identification & Pages**<br>PRO1/1008/05<br>37 p. |
| | **Date**<br>7.3.2005 |

**Report title and author(s)**

MODELLING OF THE LABORATORY EXPERIMENTS OF SOLUTE TRANSPORT THROUGH A NATURAL ROCK FRACTURE


**Summary**

This report describes first part of a two year project that examines tracer retention in solute transport through a rock fracture. The work is carried out in close co-operation with the Laboratory of Radiochemistry of the University of Helsinki, where the experimental part of the project is performed.

Objective of the whole project is to examine the processes that cause retention in solute transport through rock fractures. Especially, the focus of the work is on the matrix diffusion. The first part of the project, reported in the present report, aims to the characterisation of suitable flow fields to be used in the tracer experiment and interpretation of the pre-tests performed using non-sorbing tracers.

In the examined fracture the natural direction of the flow is towards side 3 (fracture opens towards side 3). This means that, for a maximum length of the flow path, injection should be performed in borehole KR1. This configuration has also been used in the first tracer tests that were performed using uranine, technetium and sodium.

The modelling implies that so far the flow rates have been rather high leading to advection dominated transport. Scoping calculations show that matrix diffusion begins to be observable for non-sorbing tracer when the flow rate is around 0.1 µl/min for the column experiment and around 1 µl/min for the fracture experiment.


| Distribution | Publicity |
|---|---|
| Anne Väätäinen (KTM), Kari Rasilainen (VTT/PRO), Aimo Hautojärvi (Posiva), PRO/Arkisto | FREE |

| Responsible person | Reviewed and approved by | |
|---|---|---|
| Antti Poteri<br>Senior research scientist | Lasse Koskinen<br>Group Manager | Timo Vanttola<br>Research Manager |

# ABSTRACT

This report describes the first part of a two year project that examines tracer retention in solute transport through a rock fracture. The work is carried out in a close co-operation with the Laboratory of Radiochemistry of the University of Helsinki, where the experimental part of the project is performed.

Objective of the whole project is to examine the processes that cause retention in solute transport through rock fractures. Especially, the focus of the work is on the matrix diffusion. The first part of the project, reported in the present report, aims to the characterisation of suitable flow fields to be used in the tracer experiment and interpretation of the pre-tests performed using non-sorbing tracers.

Several experiments have already been performed using the block. Hydrological properties of the fracture have been characterised by performing water flow tests in boreholes. Preliminary tracer experiments have also been conducted along the most promising flow paths and column experiments have been performed using the borehole cores of the boreholes drilled to rock block.

In the examined fracture the natural direction of the flow is towards side 3 (fracture opens towards side 3). This means that, for a maximum length of the flow path, injection should be performed in borehole KR1. This configuration has also been used in first tracer tests that were performed using uranine, technetium and sodium.

Preliminary modelling of the tests has also been carried out (Hölttä et al., 2004) and the modelling of these tests has also been revisited in this work. The modelling implies that so far the flow rates have been rather high leading to advection dominated transport.

Scoping calculations show that matrix diffusion begins to be observable for non-sorbing tracer when the flow rate is around 0.1 µl/min for the column experiment and around 1 µl/min for the fracture experiment.

# PREFACE

This work is a funded by the Finnish Nuclear Waste Research Fund. The work is carried out in a close co-operation with the Laboratory of Radiochemistry of the University of Helsinki where the experimental part of the work will be performed.

# CONTENTS

# 1 INTRODUCTION

This report describes first part of a two year project that examines tracer retention in solute transport through a rock fracture. The work is carried out in close co-operation with the Laboratory of Radiochemistry of the University of Helsinki, where the experimental part of the project is performed.

Transport experiments will be performed in a cubic block of granitic rock. The size of the rock block is about 0.6 cubic meters and it is divided by a natural fracture that has an area of about 0.9 x 0.9 $m^2$. The rock block is penetrated by nine boreholes that intersect the fracture. It also has been already instrumented for the tracer test purposes.

A set of non-sorbing tracer tests have already been conducted with the rock block. These tests are interpreted and reported by Hölttä and Hakanen (2002) and Hölttä et al. (2004). The main objective of the previous tests has been to characterise the fracture and test the experimental set-up and instrumentation. The coming tracer test program aims to observable matrix diffusion in the experimental breakthrough curves.

# 2 OBJECTIVES

Objective of the whole project is to examine the processes that cause retention in solute transport through rock fractures. Especially, the focus of the work is on the matrix diffusion. Results of this project can be used to estimate importance of the retention processes during transport in different scales and flow conditions.

The first part of the project, reported in the present report, aims to the characterisation of suitable flow fields to be used in the tracer experiment and interpretation of the pre-tests performed using non-sorbing tracers. A more complete set of tracer experiments will be carried out at the next phase of the project applying sorbing tracers. This report will also serve as guidance for the main tracer test phase.

Objectives of this phase of the project can be condensed by following points:

- Clarify the applicable flow fields to be used in the tracer experiments
- Estimate the material properties of the rock. This is performed by modelling the tracer experiments carried out with the rock columns of small scale borehole cores.
- Estimate the required flow conditions for sorbing tracer tests in order to get matrix diffusion as an observable retention process.

# 3 DESCRIPTION OF THE ROCK BLOCK

Detailed description of the rock block is given by Hölttä and Hakanen (2002). This section shortly summarises the main characteristics of the block. The rock block is medium grained grey granite and it contains a natural hydraulically conducting fracture. The size of the block is approximately 0.9 m x 0.9 m x 0.7 m and the horizontal fracture is located about 17 cm below the top of the block (see Figure 3-1 and Figure 3-2). The fracture is intersected by nine vertical boreholes. The borehole in the middle of the block has a diameter of about 3 cm and all the other boreholes are 2 cm in diameter. Locations of the boreholes are presented in Figure 3-3. The cores of the boreholes have been stored and lately they have been used in the tracer column experiments to sort out the material properties of the rock.

The rock block has been equipped with water pools that are installed at the vertical sides and top of the block. The purpose of these water pools is to ensure saturation of the block and also to stabilise the hydraulic head around the vertical faces.

The rock block is also instrumented, besides the boreholes, also at the outer vertical boundary of the block where the horizontal fracture intersects the faces of the block. One face is equipped with tracer collection cells. Preliminary tracer tests with uranine showed that migration may take place through distinct channels. The tracer collection cells are used to directly measure the breakthrough curves of the different transport channels.

*Figure 3-1. Rock block used in the experiment.*

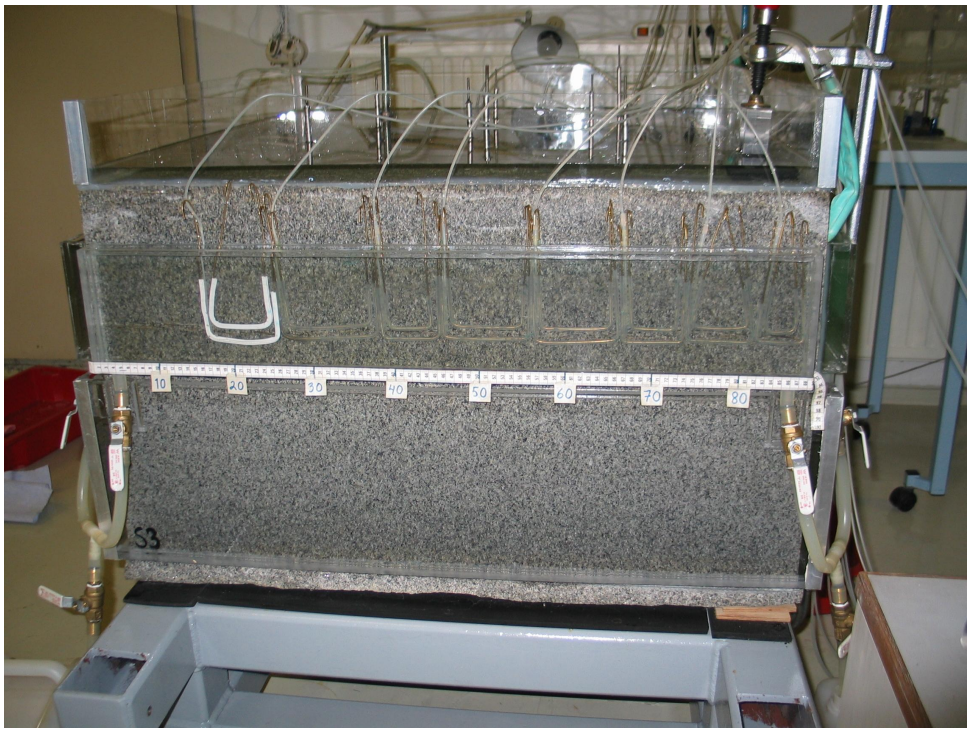


*Figure 3-2. Close-up of the tracer collection cells at the side 3 of the rock block.*

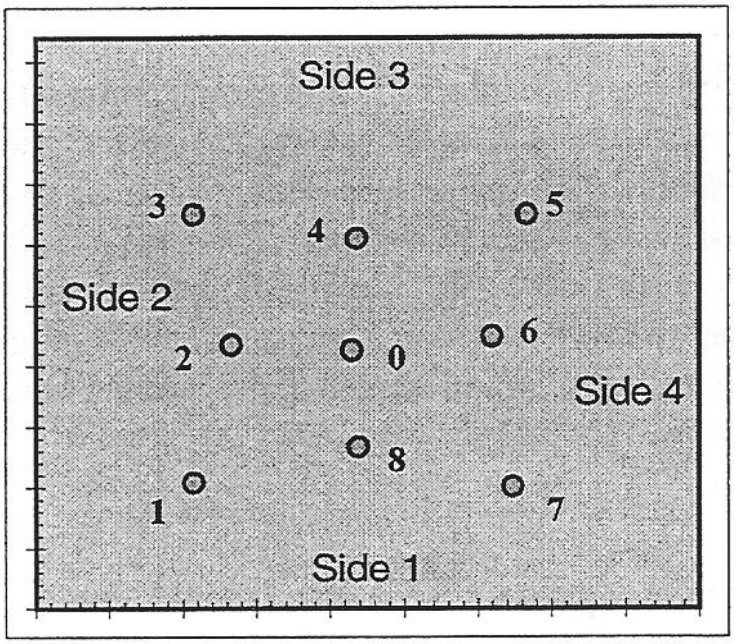


*Figure 3-3. Locations of the boreholes at the top of the block (picture from Hölttä and Hakanen, 2002).*

# 4 FRACTURE CHARACTERISATION

Several experiments have already been performed using the block. Hydrological properties of the fracture have been characterised by performing water flow tests in boreholes. Preliminary tracer experiments have also been conducted along the most promising flow paths. This section introduces shortly the characterisation experiments and revisits the modelling of one of the tracer tests. A more detailed description of the experiments can be found from Hölttä and Hakanen (2002) and Hölttä et al. (2004).

## 4.1 HYDROLOGICAL CHARACTERISATION

Hydraulic characterisation of the fracture was carried out by forcing water to one borehole at time. The pumping was performed by applying constant head in the borehole. Before hydraulic characterisation all nine boreholes were equipped with sealing packers. Water inflow to a borehole was measured as a function of the hydraulic head applied in the borehole. During testing one borehole other boreholes were sealed by the packers. The outer boundary of the fracture (at the faces of the block) was left open during the tests. However, in the interpretation of the tests the outer boundary has been treated as a constant head boundary.

In the interpretation of the pumping tests a two-dimensional flow field was assumed prevail over the fracture during the tests. In the case of radial flow the water inflow to the borehole depends on the head difference between the borehole and the outer boundary of the fracture according to following equation

$$Q = (h_w - h_o)\frac{2\pi T}{\ln\left(r_0 / r_w\right)} \quad , \qquad (4\text{-}1)$$

where $h_w$ is the head in the borehole, $h_0$ is the head at the outer boundary of the fracture, $Q$ is the water inflow rate, $r_w$ is the radius of the borehole and $r_0$ is the distance from the borehole to the outer boundary of the fracture. It can be seen from (4-1) that $Q$ versus $\Delta h=h_w-h_0$ plot should form a line, which has a slope of

$$C = \frac{2\pi T}{\ln\left(r_0 / r_w\right)} \quad . \qquad (4\text{-}2)$$

Application of this very simple model has some limitations. The outer boundary of the fracture in a cubic rock block is not strictly radial symmetric. Also, most of the boreholes are not in the middle of the block, i.e. the distance from the borehole to the outer boundary varies considerably also for this reason. However, in the radial flow field the greatest part of the friction for flow takes place in the vicinity of the pumping borehole. Therefore, simplifications made above and the locations of the borehole do not have a great influence on the results. The resulting transmissivity represents the local transmissivity around the pumping borehole. The smallest distance from the

borehole to the outer boundary has been applied as the distance to the constant head boundary ($r_0$ in equation (4-2)). It may be noted that the possible channelling of the flow can influence the transmissivities, but this is not taken into account in the interpretation of the pumping tests.

Measured water inflow for different hydraulic heads and different boreholes are presented in Figure 4-1. Fracture aperture is very small in one of the corners. Practically, the fracture is closed at the corner between side 1 and side 4 (see Figure 3-3). The aperture increases towards side 3 that can also be deduced from Figure 4-2 Boreholes 7 and 8 did not conduct water at all and they are not included in the Figure 4-1.

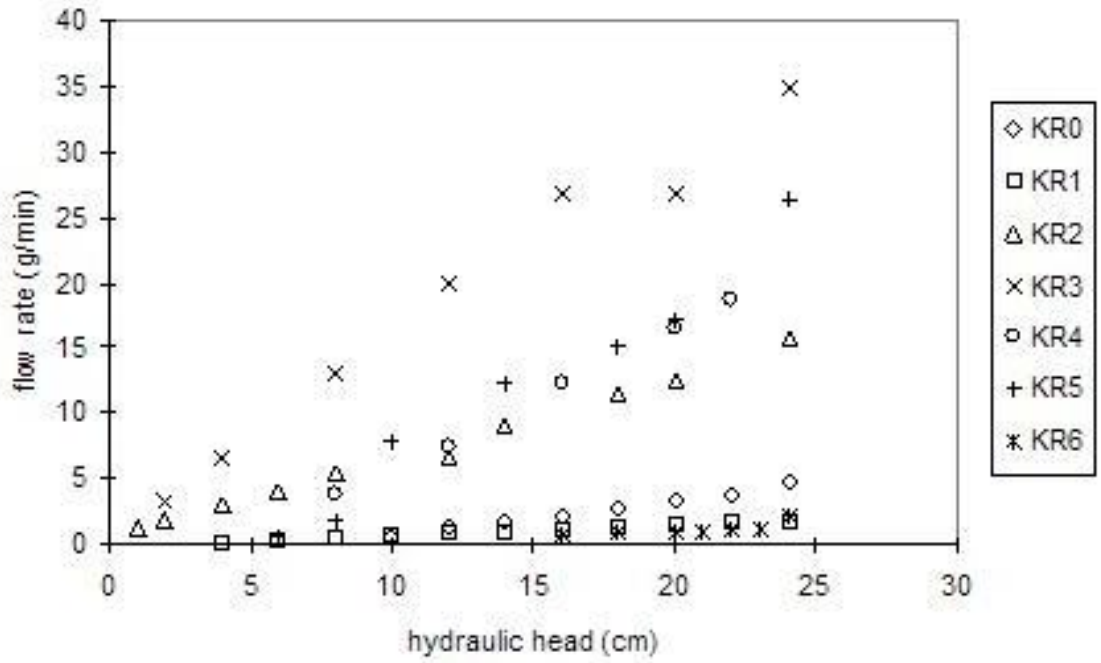


*Figure 4-1. Water inflow to the fracture at different boreholes as a function of the applied hydraulic head (based on data in Hölttä and Hakanen, 2002).*

Fitting of the line to the points in Figure 4-1 and applying equation (4-2) gives estimates of the local transmissivities around different boreholes. Figure 4-2 shows the estimated transmissivities. This figure shows clearly the increase in transmissivity (and very likely also in aperture) as the side 3 is approached. Locations of the boreholes 7 and 8 are indicated by dots although they had zero transmissivity in the tests.

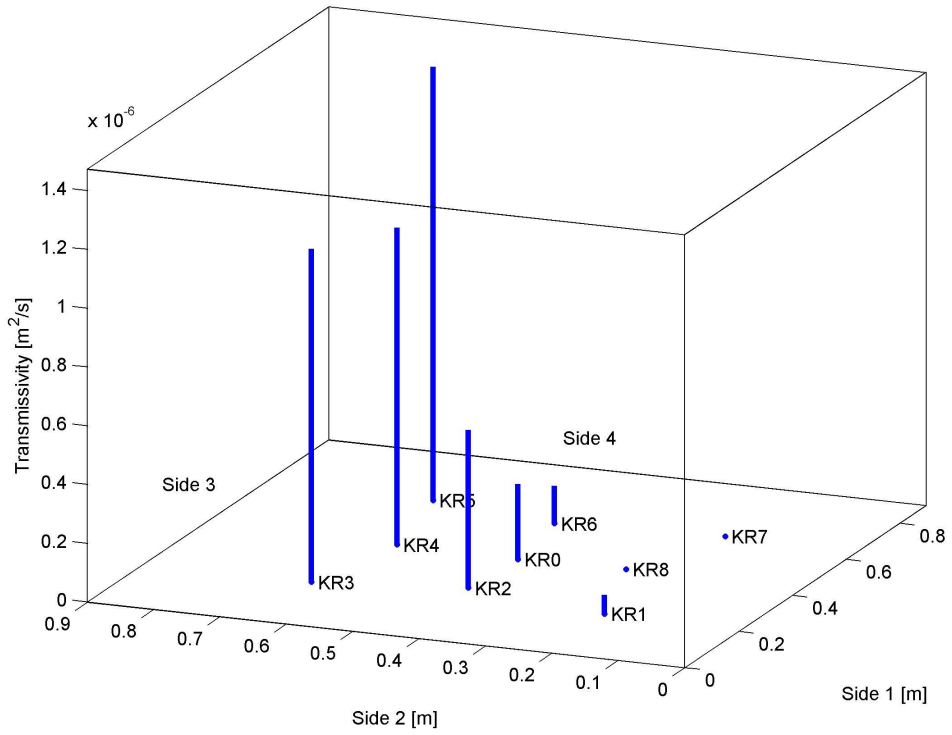


*Figure 4-2. Locations and estimated local transmissivities for different boreholes. Locations of the boreholes 7 and 8 are also indicated although they showed zero transmissivity in the test (figure is based on Hölttä et al., 2004).*

## 4.2 TRACER TESTS

After hydraulic characterisation water pools were constructed at the outer boundary of the fracture. Water pools ensure that constant hydraulic head prevails all around the outer boundary during the tracer tests. Water pools can also be used in the collection of the tracers during the tracer tests.

All tracer tests were performed in radially diverging flow field. Water was pumped to a borehole and tracer was injected to the pumped borehole. Tracer collection was made at the outer boundary of the fracture. Usually, several near-parallel flow paths were active in one test. Tracer tests were also used to identify the transport channels. Identification of the transport channels and the outflow locations at the outer boundary of the block was performed by injecting uranine from each borehole at time and recording the outflow locations at the outer boundary of the fracture.

These pre-tests show that tracer outflow locations are mainly at the side 3 (fracture opens towards side 3), but some discharge is observed also at the side 2. During construction of the water pool at the side 2 was sealed to force tracer discharge to the

side 3. The water pool at the side 3 was divided to seven adjacent tracer collection cells based on the outflow positions of the main transport channels.

The first actual tracer tests that gave an experimental breakthrough curve were carried out along the longest possible flow path on the fracture. The fracture characterisation suggested borehole KR1 as an injection borehole for these preliminary tracer tests. Two tracer experiments were performed using flow rates of 0.23 ml/min and 0.35 ml/min, respectively. Both experiments were performed by injecting tracers in KR1. In the first experiment uranine and technetium were injected using flow rate of about 0.35 ml/min. In the second test uranine, technetium and sodium were injected using flow rate of about 0.23 ml/min. In both cases the length of the flow path has been about 0.7 m. According to Hölttä and Hakanen (2002) breakthrough curves of technetium and uranine were similar. Slight retardation compared to other tracers was observed for sodium (Figure 4-3). Recovery of the tracers divided between three to four channels of the total number of seven channels. Sodium seems to spread to a wider area than technetium and uranine (Figure 4-4). Reason for this behaviour could be that the detection limit for radioactive tracer is much lower than for uranine. On the other hand, in the case of technetium the short half-life (about 6 hours) has affected the measurable recovery. However, these tests indicate that the experimental set-up is usable for tracer experiments.

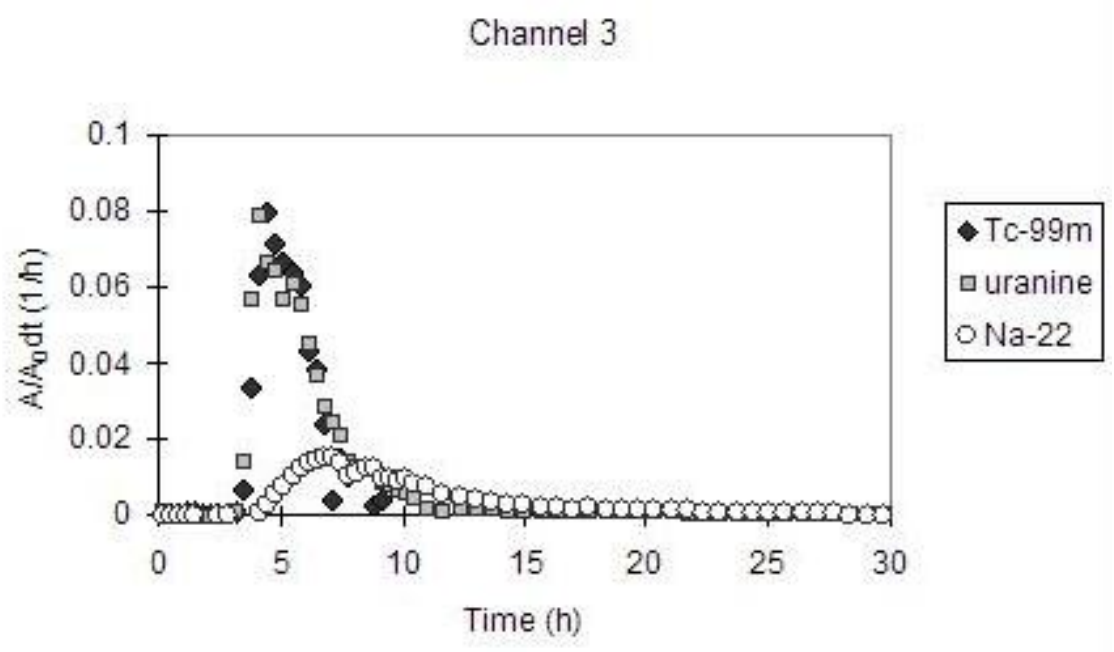


*Figure 4-3. Experimental breakthrough curves for uranine, technetium and sodium at the tracer collection cell 3 (collection cell 3 showed highest recovery).*

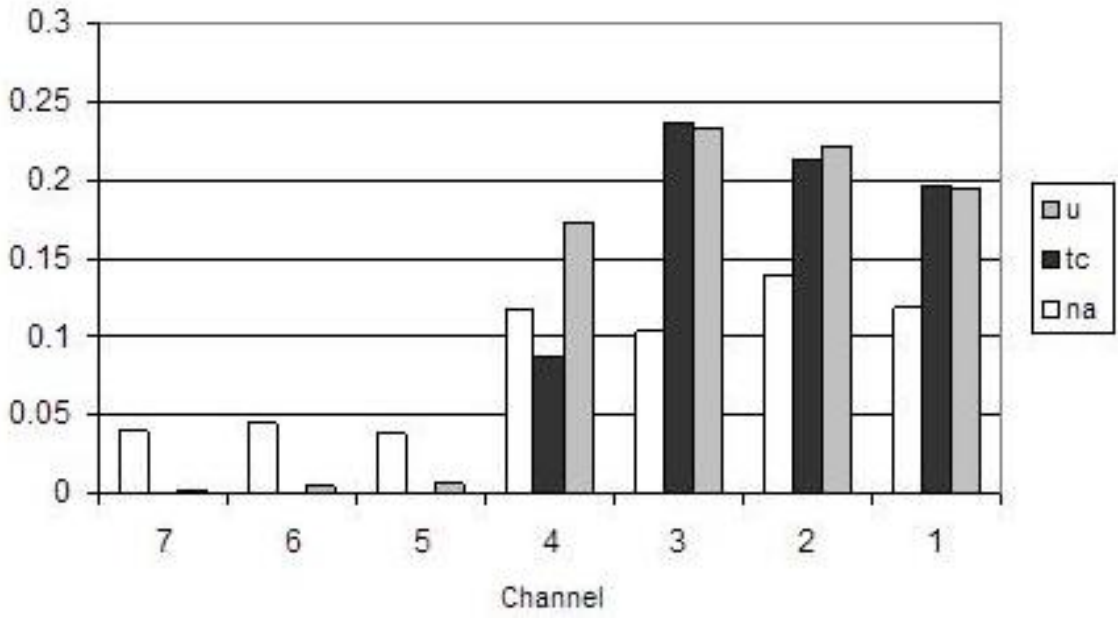


*Figure 4-4. Proportional recovery of the injected uranine, technetium and sodium at the different tracer collection cells (from Hölttä and Hakanen, 2002).*

Preliminary modelling of these tests has also been carried out (Hölttä et al., 2004). The modelling implies that the flow rates were rather high leading to advection dominated transport. Previous modelling was revisited in this work. Resulting characterisation of the transport channel and flow field is presented in Table 4-1. Properties of the transport channel are based on the geometric considerations. Recovery has been observed over about 40 cm region at side 3, which gives average 20 cm width of the channel. Mean Aperture of the channel comes from the measured transmissivities. Correlation length of the velocity field and the ratio of hydraulic to transport aperture ($C_v$) have been used as fitting paramters.

Modelled and experimental breakthrough curves for uranine in the tracer collection cell 3 are presented in Figure 4-5. Conclusion of the present modelling is the same as the previous modelling, i.e. that the tracer transport is dominated by the advection. The current model includes also matrix diffusion, but it is not cannot be seen in these experimental results. Observable matrix diffusion requires much smaller flow rates for this experimental set-up.

*Table 4-1. Parameters used to model the tracer experiment with the advection-Taylor dispersion-matrix diffusion model.*

| **Parameter** | **Value** |
|---|---|
| Flow rate to channel | 350 and 230 µl/min |
| $C_v$ (transport to hydraulic aperture ratio) | 5.6 |
| Channel width | 20 cm |
| Channel length | 70 cm |
| Channel volume (hydraulic) | 13.5 ml |
| Correlation length of the velocity variation | 0.9 cm |
| Rock porosity | 0.2% |
| Rock density | 2600 kg/m$^3$ |
| Rock pore diffusivity | $2.4 \cdot 10^{-11}$ m$^2$/s |
| Diffusivity in free water | $10^{-9}$ m$^2$/s |
| Volume of tubing | Estimated delay in tubings (23 min and 20 min) subtracted from the measured breakthrough curves |

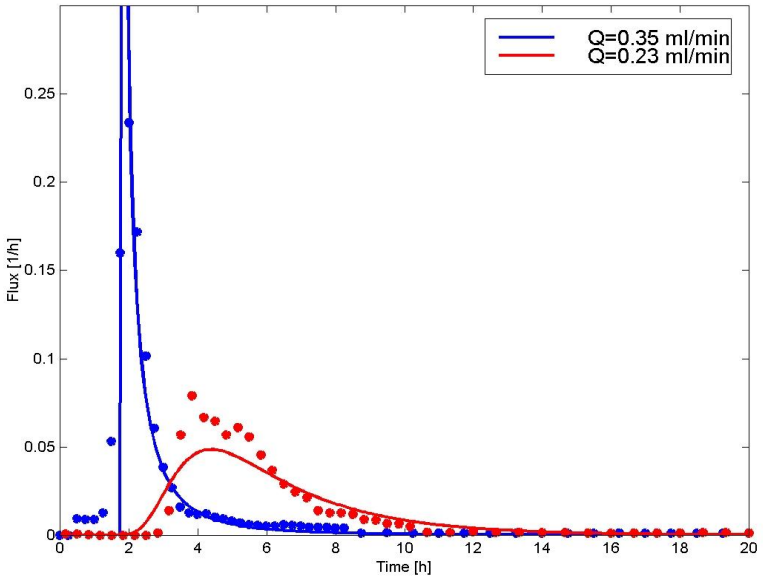


*Figure 4-5. Modelled and measured breakthrough curves for uranine. Breakthrough curves are presented for the tracer collection cell 3. Parameters used in the modelling are given in the Table 4-1.*

# 5 COLUMN EXPERIMENTS USING ROCK BLOCK MATERIAL

The fracture in the rock block has been intersected by nine boreholes. The borehole cores have been glued one after the other to form two rods, one is 74.5 cm long and another is 68.5 cm long. Rods have been used in a column experiment to sort out transport properties of the rock material. The diameter of the borehole core is 14 mm. It is placed inside a tube that has an inner diameter of 15 mm. This leaves 0.5 mm gap between the core and the tube. This section discusses the tracer tests carried out using the longer, 74.5 cm, column.

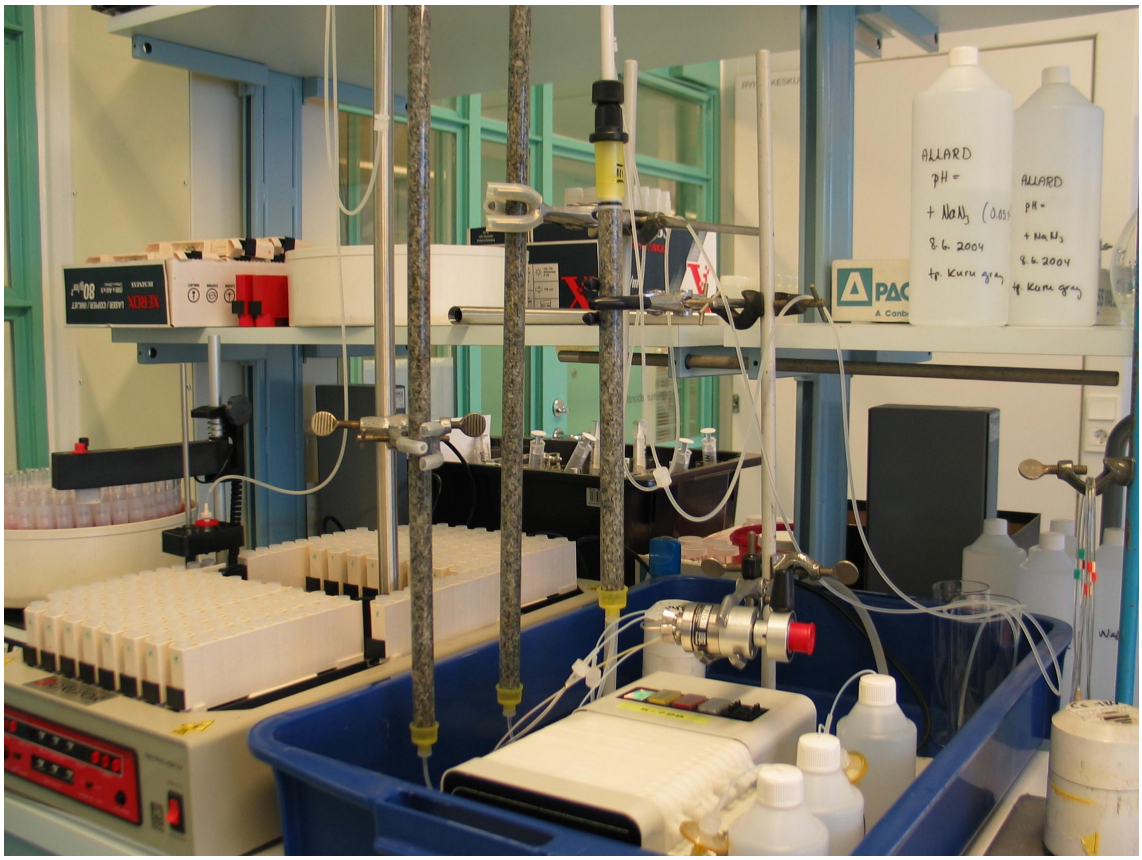


*Figure 5-1. Borehole cores were used for rock columns. Tracer tests have been carried out using the columns.*

Model calculations have been performed to estimate the retention time and spreading of the breakthrough pulse that is caused by matrix diffusion for different parameter combinations. Retention is characterised by the time of the peak of the calculated breakthrough curves (without advective delay) and half-width of the breakthrough curve. Figure 5-2 shows the matrix diffusion retention time and the spreading of the breakthrough curve as a function of the rock porosity and flow rate through the column. These calculations have been made applying Cartesian geometry, not the actual cylindrical geometry, but the limited volume of the borehole core has been taken into

account. In the calculations the thickness of the rock has been 4 mm. The 4 mm layer at the surface of the borehole core corresponds to quite significant part of the borehole core. The 4 mm layer at the surface of the core gives about 82% of the total volume of the core. This indicates that if the present model show effects of the limited volume of the rock matrix then it can be concluded that also the actual cylindrical system will be affected by the effects of the limited core volume. The influence of the limited volume of the rock can be seen in Figure 5-2 as a change in the slope of the surface that takes place around the yellow region (from square to linear dependence, the figure is in log-scale). Naturally, the Cartesian model can be used for the weak matrix diffusion cases, because the penetration depth to the rock matrix is so small that the column looks infinite for the tracer particles.

It is known from the other measurements that the porosity of the rock is likely to be closer to the lower limit of the range shown in Figure 5-2 (0.2%). Thus, it seems that matrix diffusion begins to be an observable phenomenon if the flow rate through the column is lower than 0.1 µl/min. On the other hand the limited volume of the column begins to influence the results at flow rates that are smaller than 0.01 µl/min.

The volume of the flow channel in the column is about 17 ml and tubing takes about 1.3 ml. This means that the advective delay for a flow rate of 0.1 µl/min will be about 4 months.

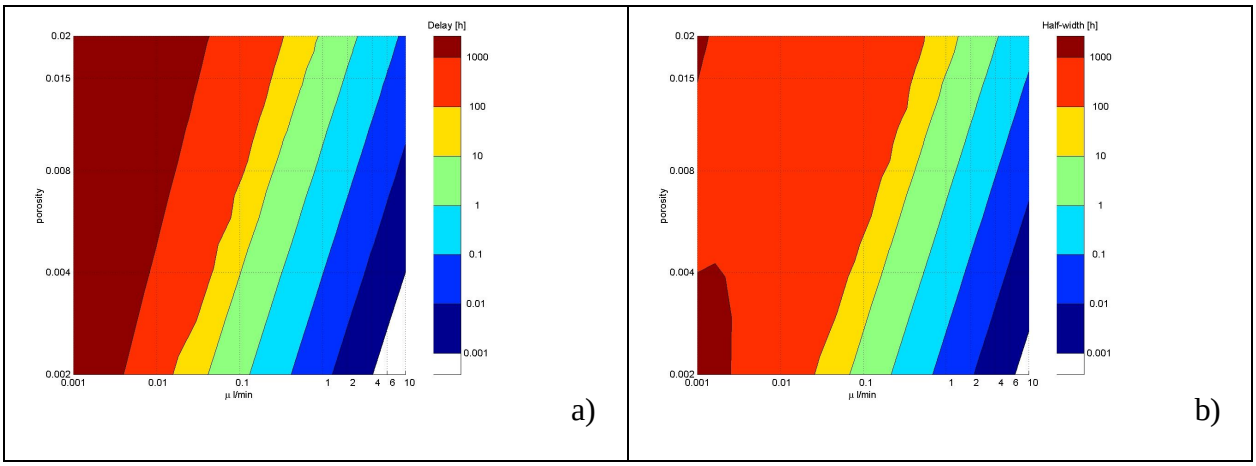


*Figure 5-2. The colour scales represents retention time caused by matrix diffusion for an instantaneous release of tracer (a) and the half-width of the breakthrough curve (b), when the flow rate through column and the porosity of the rock are varied.*

At the moment four tests have been performed using tritium (HTO) and one test using sodium. Applied flow rates vary from about 6 µl/min to 47 µl/min. This offers an opportunity for the first test that is simple scaling of the breakthrough curves by the applied flow rates. In Figure 5-3 the breakthrough curve of the highest flow rate is scaled to get it to correspond to the measured lower flow rates. There is a good agreement between shapes of the curves. This result supports quite strongly the interpretation that these tests were advection dominated.

It may also be noted that the two tests performed with the flow rate of 10 µl/min show different breakthrough curves. This indicates the repeatability and sensitivity of these tests.

It has also been possible to model these tests by assuming linear velocity profile and Taylor dispersion and using parameters that are given in Table 5-1. The fitting to the measured breakthrough curves was done by changing $C_v$ (ratio between transport and hydraulic aperture) and the correlation length of the velocity variation. Any effects of the matrix diffusion cannot be seen in the results although it has been incorporated to the model (Figure 5-4).

*Table 5-1. Parameters used to model the tracer experiment with the advection-Taylor dispersion-matrix diffusion model.*

| **Parameter** | **Value** |
|---|---|
| Flow rate to channel | 6, 10 and 47.4 µl/min |
| $C_v$ (transport to hydraulic aperture ratio) | 1.5 |
| Channel width | 4.4 cm |
| Channel length | 74.5 cm |
| Channel volume (hydraulic) | 17 ml |
| Correlation length of the velocity variation | 0.75 cm |
| Rock porosity | 0.2% |
| Rock density | 2600 kg/m$^3$ |
| Rock pore diffusivity | $2.4 \cdot 10^{-11}$ m$^2$/s |
| Diffusivity in free water | $10^{-9}$ m$^2$/s |
| Volume of tubing | 1.27 ml |

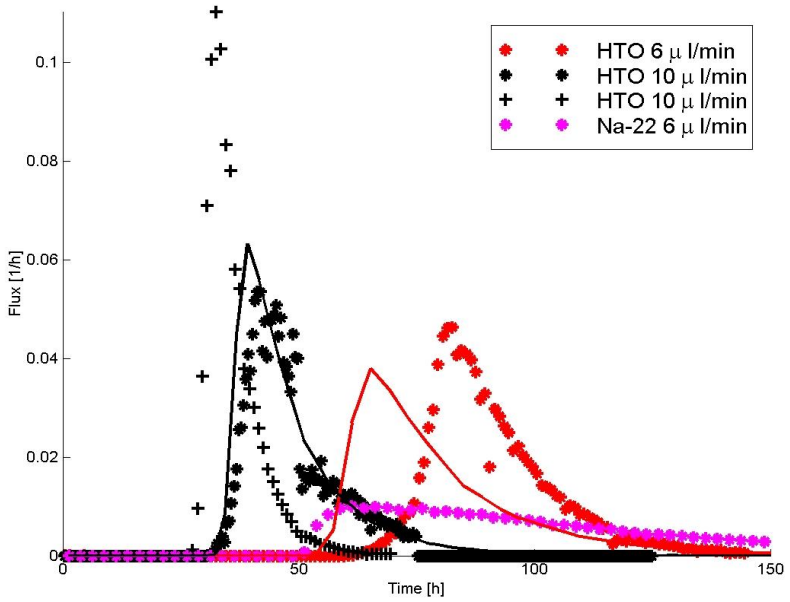


*Figure 5-3.Breakthrough curves for the column experiments carried out with the cores of the boreholes. Markers indicate measured breakthrough curves for 10 µl/min and 6 µl/min experiments. Solid lines show the measured breakthrough curve for 47.4 µl/min flow rate that is just scaled to indicate 10 µl/min and 6 µl/min flow rates.*

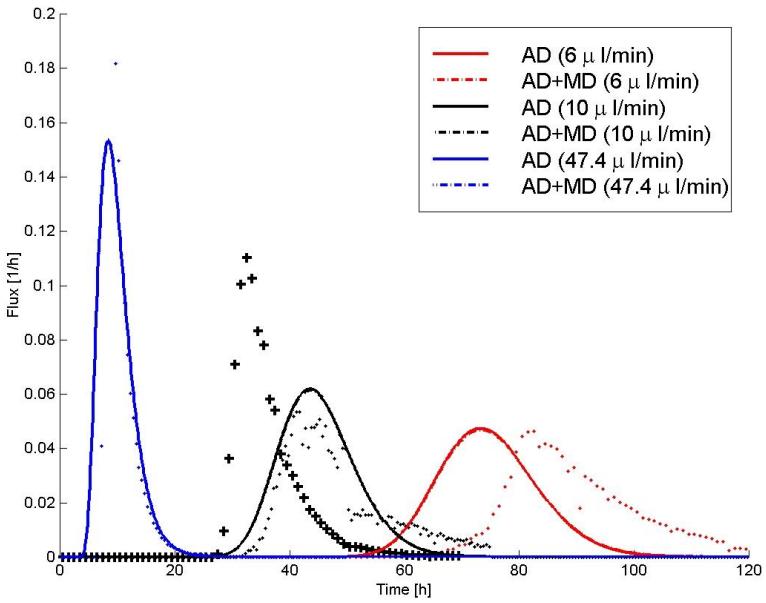


*Figure 5-4. Modelling results for the column experiments carried out with the cores of the boreholes. Applied parameters are presented in Table 7-1. Note that in these tests modelled breakthrough curves with matrix diffusion cannot be distinguished from the breakthrough curves without matrix diffusion.*

# 6 FLOW PATHS IN THE FRACTURE

In this section the hydraulic characterisation and flow path tests with a tracer (uranine) are revisited to determine the structure of the flow channels in the fracture. First an overall picture of the flow paths is formed using results from all boreholes at the same time. Then stability of the flow conditions and flow channels is studied by examining each borehole and each test separately.

## 6.1 CHANNELLING

Large numbers of flow path tests, with and without a tracer, were performed after the boreholes were drilled. Flow tests were performed by pumping water to one borehole at time and then observing the outflow locations of the water or tracer at the outer boundary of the fracture.

After construction of the water pools around the block the flow path tests were performed using uranine as a tracer. These tests were conducted in the similar way as the tests with water only. Water was pumped to one borehole at time. Some of the water was labelled using a pulse of uranine and outflow locations of the uranine at the outer boundary were recorded using a video camera (Hölttä and Hakanen 2002).

Two sets of flow tests and one set of tests with the tracer were conducted. One set of tests may contain several repeated tests from the same borehole. Results of all these tests are summarized in Figures 6-1 and 6-2 for the flow tests and in Figure 6-3 for tests with a tracer. Results of the flow tests and tests with a tracer are presented in a plan view over the fracture. Lines connect each water inlet position (borehole) to the corresponding outflow positions. Flow channels representing each tested borehole are in different colours. This does not give precise information on the flow channels but it indicates possible anisotropies over the fracture plane.

The overall trend in Figures 6-1 to 6-3 indicates the increase in fracture aperture when side 3 is approached. Transmissivity in two of the boreholes close to side 1 was so low that it was not possible to perform tests in them (KR7 and KR8). The distribution of flow paths seems to be more isotropic for boreholes close to the side 3 and anisotropic close to side 1. For example, borehole KR1 that is close to side 1 shows clearly channelised behaviour. In this case flow paths are formed towards side 1 and side 3, but not towards side 2 although the distance from KR1 to side 2 is short.

Comparison between flow tests (Figures 6-1 and 6-2) and tests with a tracer (Figure 6-3) shows that with a tracer flow paths favour direction towards side 3 more than in the flow tests. This may be explained by the sensitivity of the tracer transport on the flow rate. Flow paths towards side 3 have much larger flow rate than other flow paths and therefore they also carry majority of the tracer causing the amount of tracer along other possible flow paths to be under the detection limit. Note that, detection of the uranine in these tests was made only visually. In flow tests only the presence of water (moisture), not flow rates, were recorded. There is also another potential explanation for the differences between flow tests and tests with a tracer. The hydraulic head applied in the tests with a tracer was about 110-120 cm as it was only about 20 cm in the flow tests. There is only about 17 cm rock above the fracture and that the upper part of the block is loose all-over but one corner. In principal, the hydraulic head applied in the tests with a tracer is strong enough to open the fracture slightly. Especially, the opening of the fracture would affect apertures at side 3 increasing the difference in transmissivity between areas close to side 1 and side 3, respectively. As a summary, it is seems evident that flow paths towards side 3 are the major flow paths for the tracer tests.

An interesting detail regarding the heterogeneity of the fracture can be concluded from both flow tests and, especially, from transport tests. Pattern of the interpreted transmissivities from different boreholes shows that the aperture of the fracture increases not straight towards side 3, but diagonally towards the corner of the side 2 and side 3. Pattern of the directions of the flow paths in Figure 6-3 shows two main orientation of the channelling. The main channels are more or less perpendicular to the gradient of the fracture aperture and another set of channels that is parallel to the gradient of the fracture aperture.

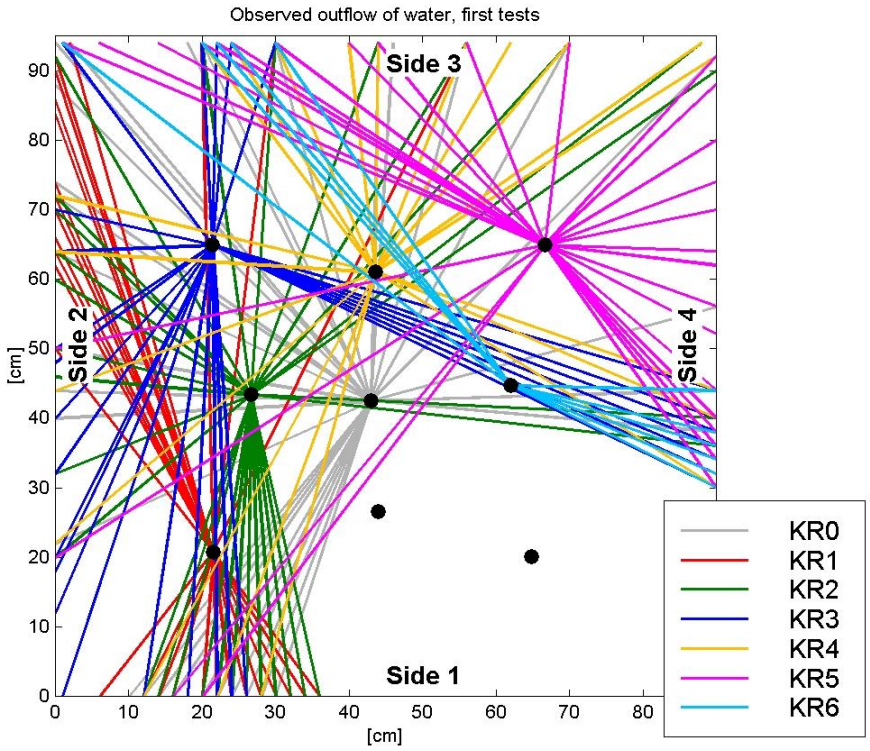


*Figure 6-1. Outflow locations of water at the outer boundary of the block for the first hydraulic tests. Locations of the boreholes are indicated by black dots. Pumped borehole and corresponding outflow locations are connected by straight line to indicate the flow path (cf. the legend).*

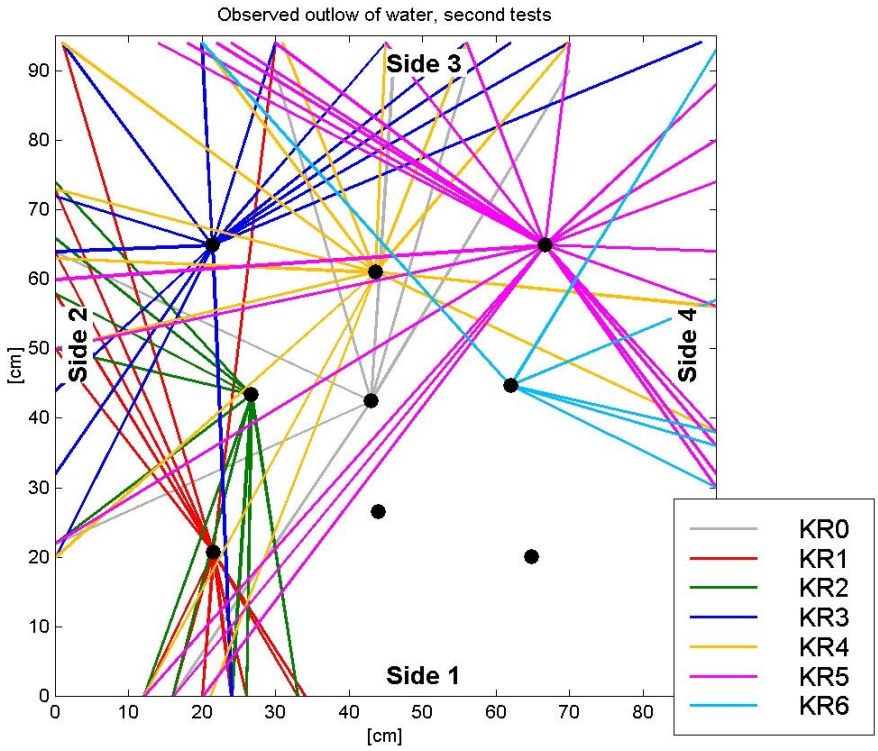


*Figure 6-2. Outflow locations of water at the outer boundary of the block for the second hydraulic tests. Locations of the boreholes are indicated by black dots. Pumped borehole and corresponding outflow locations are connected by straight line to indicate the flow path (cf. the legend).*

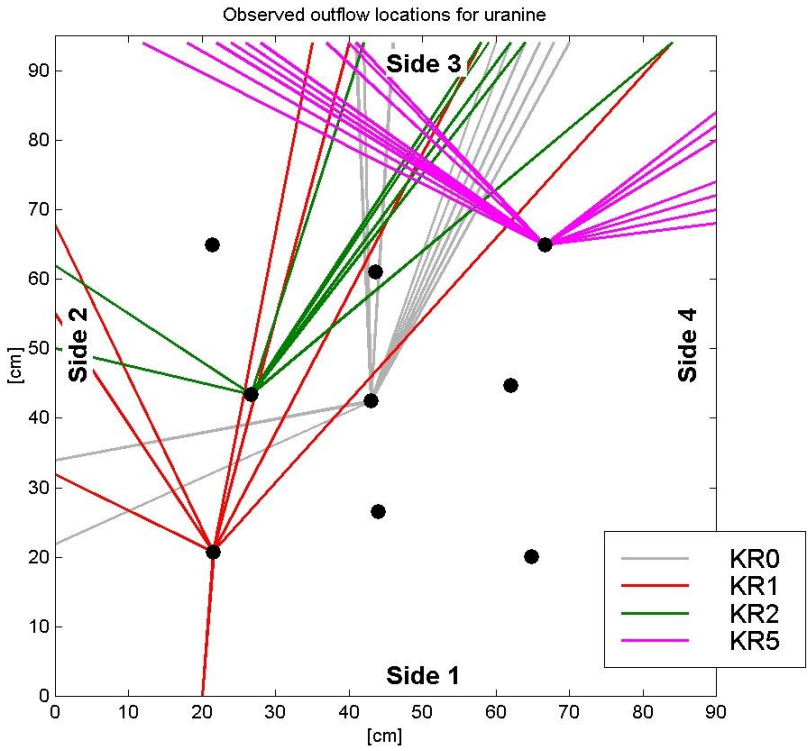


*Figure 6-3. Outflow locations of uranine at the outer boundary of the block. Locations of the boreholes are indicated by black dots. Uranine has been injected to the pumped borehole. Pumped borehole and corresponding outflow locations are connected by straight line to indicate the flow path. Results for each borehole are represented by different colours (cf. the legend).*

## 6.2 STABILITY OF THE FLOW PATHS

Stability of the transport channels is examined by comparing the patterns of flow paths for repeated tests of same experimental configuration. Precise location of the transport channels inside the fracture cannot be determined, but it is possible to illustrate the main directions of the flow paths. This is done by connecting the inflow and outflow locations of the flow paths by straight lines in the same way as in the previous section, but now separately for each test. Flow channels are reflected in the patterns of the lines.

The amount of repeated tests varies between boreholes. Two different sets of flow tests and one set of tests with a tracer were performed. Tests with a tracer were carried out only for boreholes KR0, KR2 and KR5.

Tests carried out in each borehole are presented in Figures 6-4 to 6-10. Generally, flow fields seem to be more isotropic in the first flow tests than in the second flow tests, or especially, in the tests with a tracer. It seems also that in the second set of water flow tests the flow paths through low transmissivity regions change or disappear (in figures these flow paths go towards right hand side or towards lower right corner of the block).

Tests with a tracer are more sensitive to the differences in transmissivity and flow paths towards side 1 are not observed in these tests. The observed changes in the patterns of the flow paths show that some changes of the flow paths may take place between different tests. However, for a high flow rate path that goes through a high transmissivity region of the fracture (i.e. towards side 3) the repeatability of the experiment is good.

If different boreholes are compared then most stable flow paths were obtained for KR0 and KR1. Borehole KR6 is an opposite example where the flow paths concentrate around two direction in first tests, but spread more in the second tests.

Below is shortly commented how different test configurations behave if repeated tests are compared.

- KR0: Consistent results among the tests. Same features can be seen both in tests with a tracer and water flow tests, but the directional spread of flow paths in flow tests is more uniform than in the tests with tracers.
- KR1: Only flow tests available. Consistently the same pattern of flow paths in all tests.
- KR2: Significant differences between the two sets of water flow tests. Flow paths to side 3 and side 4 are missing from second tests. Two tests with tracer. These tests have the same pattern, which is a subset of flow paths of first water flow tests.
- KR3: Only flow tests available. Flow paths change in the low transmissivity region. Flow paths to side 4 are missing in the second flow tests.
- KR4: Only water flow tests available. Consistent results between the tests.
- KR5: Tests with tracer show different character than flow tests. Flow paths of tests with tracer are a subset of flow tests. Repeated flow tests and tests with a tracer show very consistently the same pattern, respectively.
- KR6: Only flow test available. Small changes between tests. In the first tests paths concentrate around two directions, but spread more in the second tests.

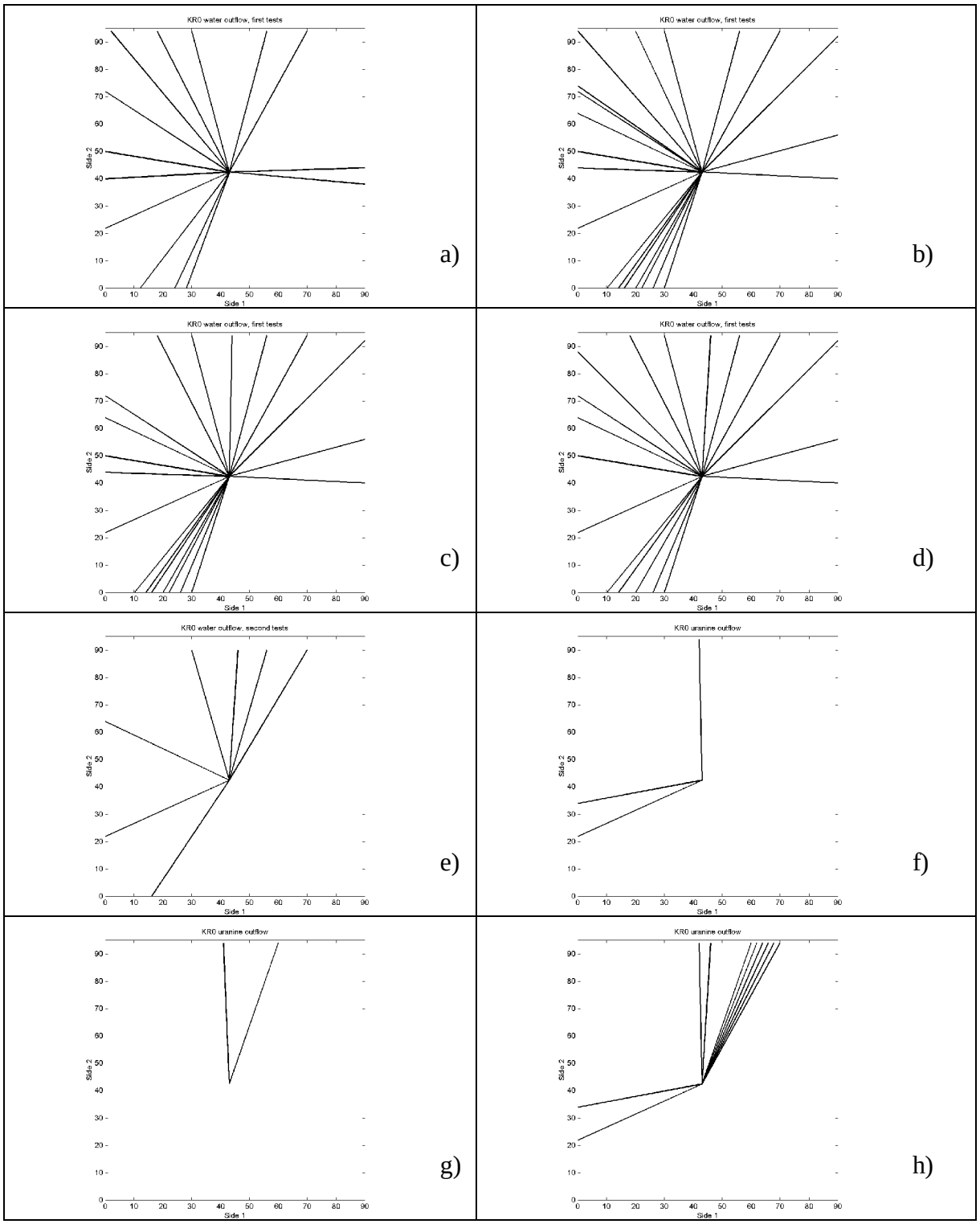


*Figure 6-4. Illustration of the flow paths when KR0 is used as a source. Figures from a) to e) are based on observations of the water outflow locations and figures from f) to h) are based on observation of the tracer (uranine) outflow locations at the outer boundary of the block. Flow paths are indicated by connecting the outflow locations to the pumped borehole with a straight line.*

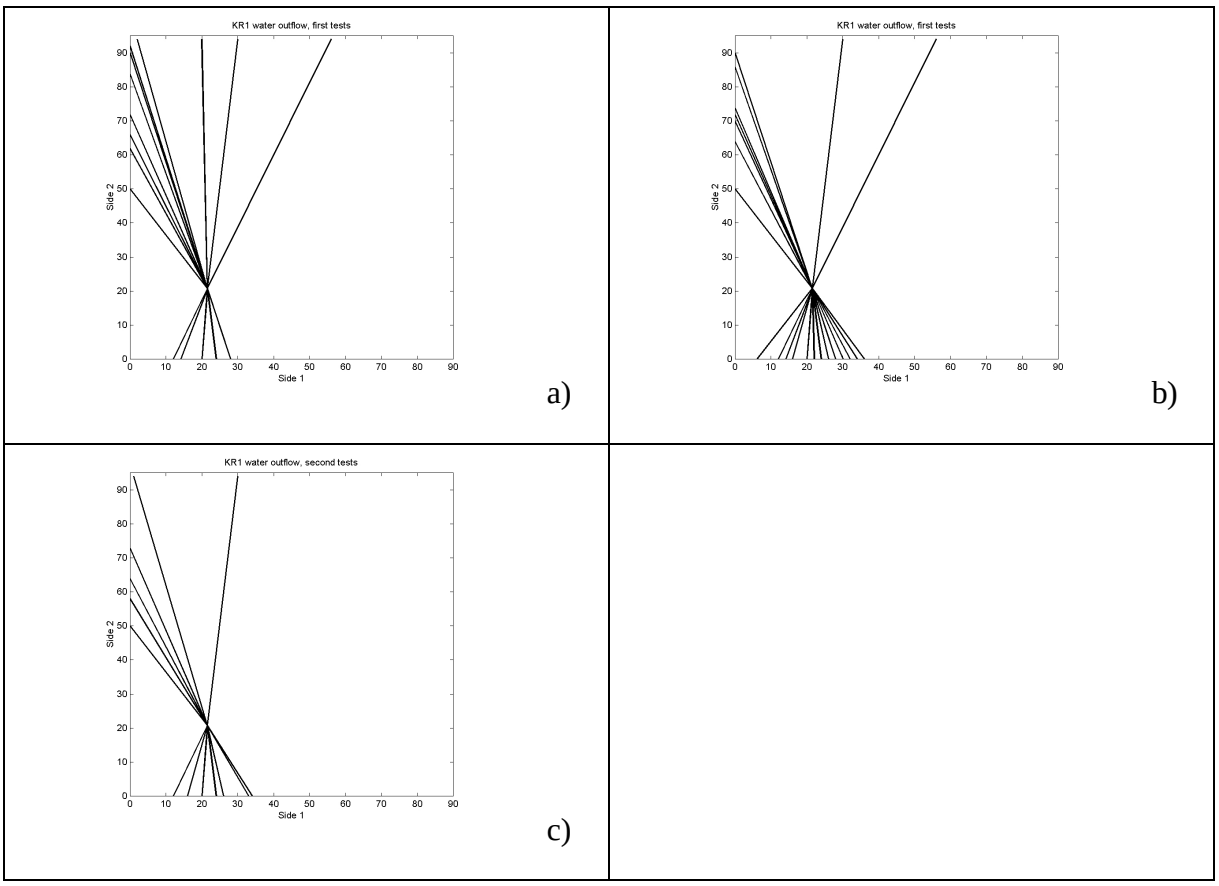


*Figure 6-5. Illustration of the flow paths when KR1 is used as a source. All figures are observations of the water outflow locations at the outer boundary of the block. Flow paths are indicated by connecting the outflow locations to the pumped borehole with a straight line.*

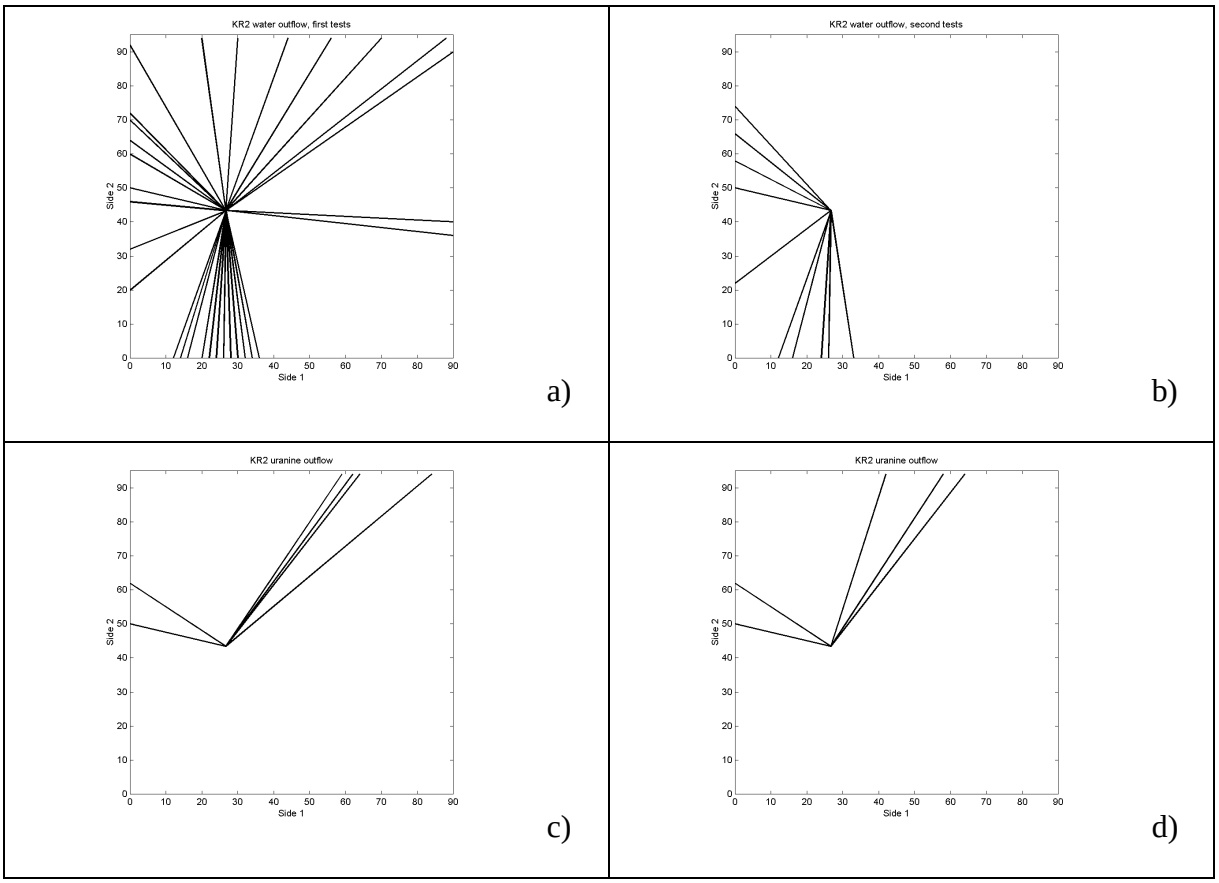


*Figure 6-6. Illustration of the flow paths when KR2 is used as a source. Figures a) and b) are observations of the water outflow locations and figures c) and d) are observations of the tracer (uranine) outflow locations at the outer boundary of the block. Flow paths are indicated by connecting the outflow locations to the pumped borehole with a straight line.*

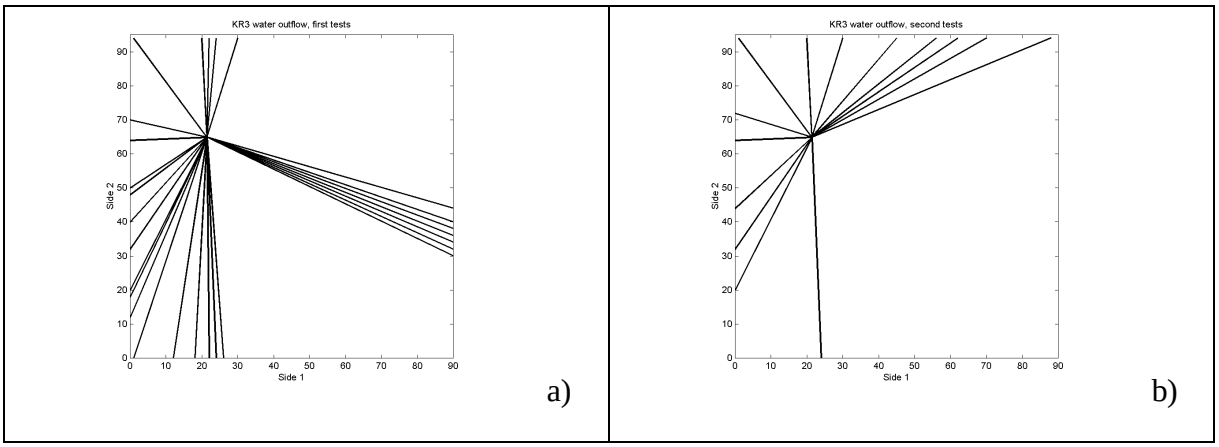


*Figure 6-7. Illustration of the flow paths when KR3 is used as a source. All figures are observations of the water outflow locations at the outer boundary of the block. Flow paths are indicated by connecting the outflow locations to the pumped borehole with a straight line.*

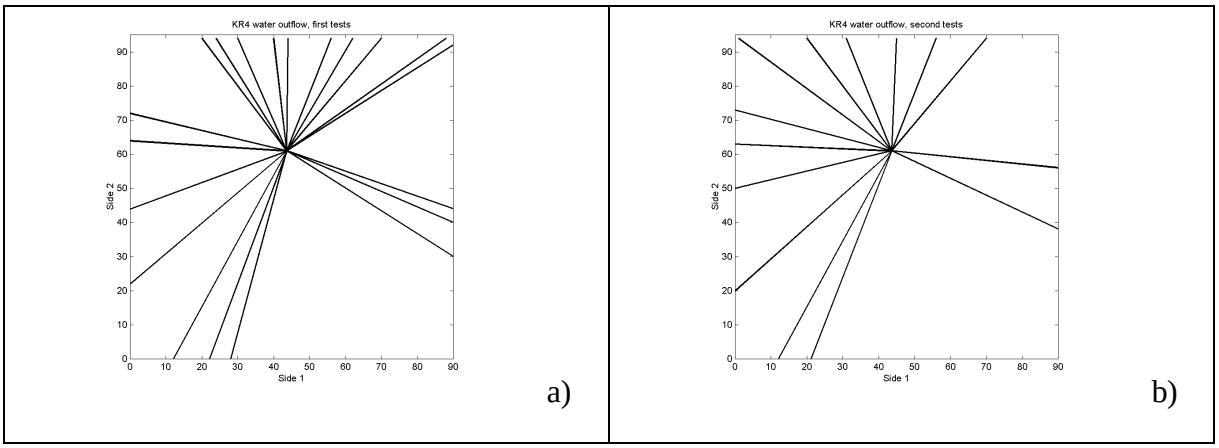


*Figure 6-8. Illustration of the flow paths when KR4 is used as a source. All figures are observations of the water outflow locations at the outer boundary of the block. Flow paths are indicated by connecting the outflow locations to the pumped borehole with a straight line.*

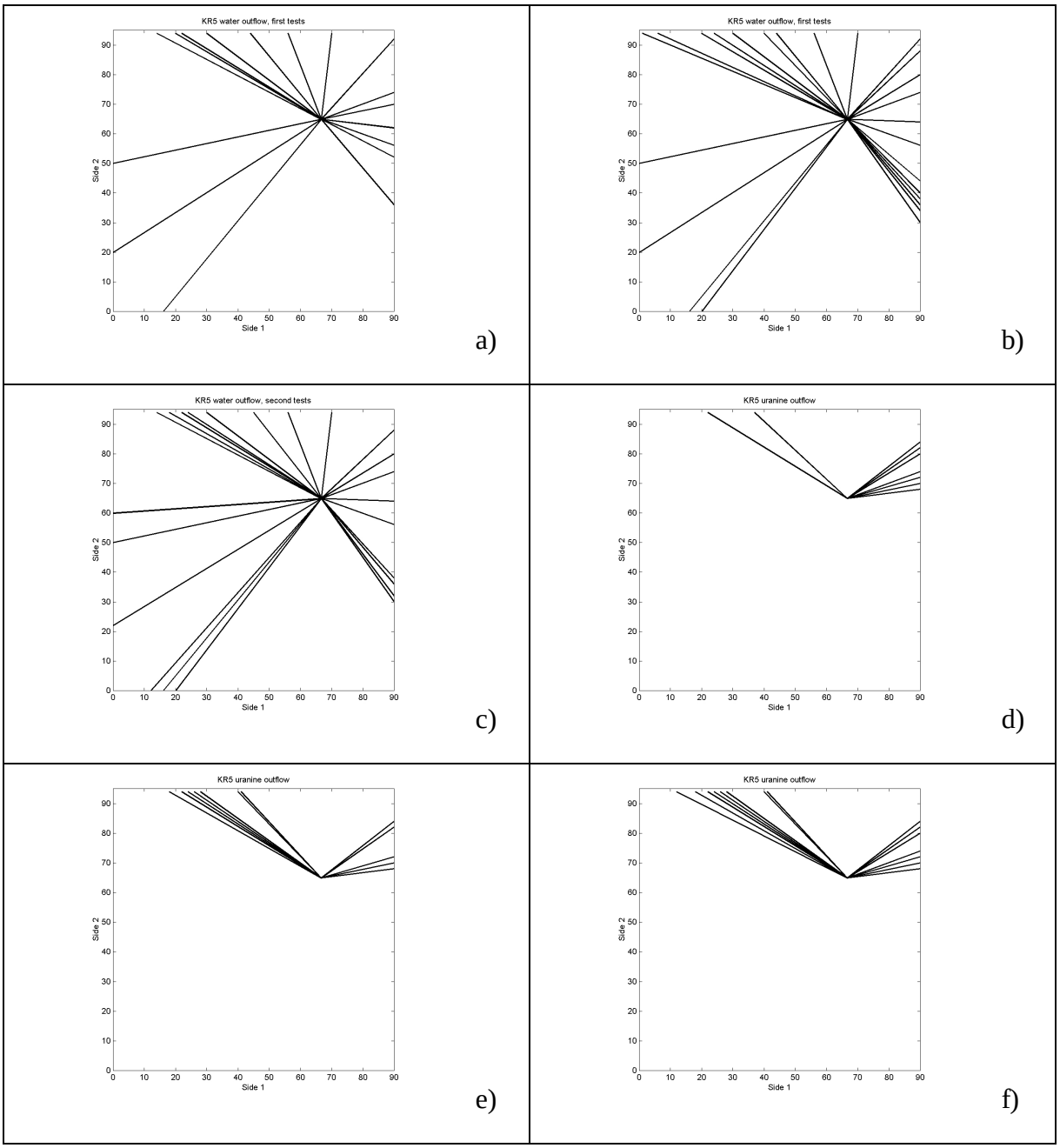


*Figure 6-9. Illustration of the flow paths when KR5 is used as a source. Figures a), b) and c) are observations of the water outflow locations and figure d), e) and f) are observations of the tracer (uranine) outflow locations at the outer boundary of the block. Flow paths are indicated by connecting the outflow locations to the pumped borehole with a straight line.*

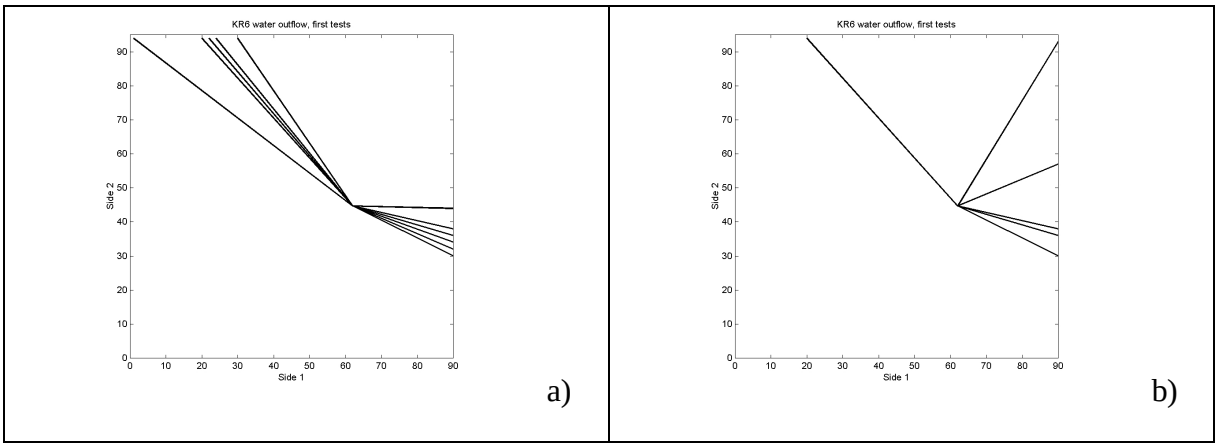


*Figure 6-10. Illustration of the flow paths when KR6 is used as a source. All figures are observations of the water outflow locations at the outer boundary of the block. Flow paths are indicated by connecting the outflow locations to the pumped borehole with a straight line.*

## 6.3 POSSIBLE FLOW PATHS IN THE FRACTURE TESTS

Tracer experiment should be made along flow paths that enable investigation of the matrix diffusion. Influence of the matrix diffusion to the tracer migration depends both on the properties of the rock and flow field. The flow field part is governed by a grouped entity, WL/Q. This means that the importance of matrix diffusion increases for long flow paths and low flow rates.

In the examined fracture the natural direction of the flow is towards side 3. This means that, for a maximum length of the flow path, injection should be performed in KR1. This configuration has been used in the first tracer tests that were performed using uranine, technetium and sodium. Mapping of the flow paths show that KR1 is close enough to side 2 so that significant part of the injected tracer could leak out through side 2 (Figure 6-5). In the present instrumentation of the block side 2 is sealed to avoid short-cutting of the flow path from KR1 to the side 2. This should also be the case in the coming tracer tests.

Alternative shorter flow paths can be tested by using boreholes KR0 or KR2. The long duration of the tests (due to the low flow rates) probably does not allow completely separate tests from these boreholes. However, one option could be simultaneous injection of different tracers both in KR1 and KR0 or KR2. Advantages of this configuration are that during one experiment it could be possible to study a shorter and longer leg of the same flow path. Note, that flow paths from KR1 and KR0 or KR2 probably share some of the channels that end up at side 3 (cf. Figure 6-3). Disadvantages are that injection at two boreholes in the same tests may complicate the determination of the flow field.

# 7 REVISIT OF THE EXISITING TRACER TEST AND SUGGESTED TEST PARAMETERS

Equivalence between the column and fracture flow experiments can be estimated from quantity *u,* which controls the matrix diffusion interaction

$$u = \varepsilon \sqrt{D_p R_p}\,\frac{WL}{Q}\ , \qquad (7\text{-}3)$$

where $\varepsilon$ is the rock porosity, $D_p$ is the pore diffusivity, $R_p$ is the retardation coefficient in the rock matrix, $L$ is the length of the transport path and $Q/W$ is the flow rate per width in the transport channel. It may be assumed that differences between the column experiments with the borehole cores and fracture are only in the flow field i.e. the last part, $WL/Q$, of the equation (7-3). Of course, if the applied flow rates are extremely low the small volume and cylindrical geometry of the boreholes cores begin to influence the results of the column experiment. However, these flow rates are probably too low (less than 0.01 µl/min based on Figure 5-2) for a realistic experiment and these effects are not taken into account in this discussion.

It appears that the length of the transport path along the fracture from borehole KR1 to the side 3 is about as long as the borehole core in the column experiments (ca. 70 cm). In this case the difference in WL/Q between the column and fracture tests arises only from the quantity Q/W.

First, we compare the estimated channel widths of the column and fracture tests. In the column experiment the maximum channel width is the perimeter of 1.4 cm borehole core, i.e. about 4.4 cm (for diffusion in water $\sqrt{2D_w t_w} = 2.2\,\text{cm}$ in 67 hours, corresponding to a flow rate of 4.2 µl/min through the column).

The tracer tests performed in fracture showed that water and tracer injection in KR1 cause tracer recovery in, at least, collection cells 1-4 (total width about 35-40 cm). For sodium the spreading of the tracer has been even larger (cf. Figure 4-4). The maximum recovery collected in one tracer collection cell has been about 25% of the injected mass (collection cell 3). In these tracer tests the flow field have been radial diverging: tracer and water injection in borehole KR1 and collection at the outer boundary of the fracture (side 3). First approximation of the flow field is that the width of the channel increases linearly from about 1.5 cm (at borehole) to about 35-40 cm (at the tracer collection boundary). If the flow is uniformly distributed or tracer is well mixed by diffusion over the whole channel width then WL/Q of the channel can be calculated using effective (average) width of channel, total flow rate and channel length (these assumptions need to be revisited when the results of the coming tracer test are evaluated). In this case we may also use average of W/Q along the flow path. From matrix diffusion point of view the flow field of a tracer test can be replaced by constant width channel that is 18-21 cm wide (average of 1.5 and 35-40 cm). This indicates that about four times higher flow rates can be used in the fracture tests than in the column experiment and still the effect matrix diffusion to the breakthrough curve should be similar.

Scoping calculations have been made for both column and fracture experiments. Basis of the scoping calculations is the geometrical discussion above. In addition, the evaluation data from the existing column and fracture tests have also been used (see Table 7-1). Existing column and fracture tests are dominated by the advective field and correspondingly the processes taking place in the advective field (diffusional mixing). Scoping calculation for both column and fracture experiment were carried out using the tracer test models, but only decreasing the flow rates (Table 7-1).

These calculations show that matrix diffusion begins to be observable for non-sorbing tracer when the flow rate is around 0.1 µl/min for the column experiment (Figure 7-1) and around 1 µl/min for the fracture experiment (Figure 7-2). The scoping calculations of the fracture experiment were carried out also for a slightly sorbing tracer (sorption is taken into account only inside the pore space of the rock, i.e. no surface sorption). Clearly, sorption in rock matrix increases the influence of the matrix diffusion on the breakthrough curve.

Note, that the based on the results of the existing tracer tests it is not possible to give completely unique values for model parameters. The advection governed tests are sensitive to the transport porosity ($C_v$·hydraulic volume) and the shape of the curve to the velocity profile (correlation length of it). In the scoping calculations the geometry of the channel (the effective width of the channel that will influence the matrix diffusion) is based only on the geometrical consideration that is presented in this section.

*Table 7-1. Parameters used to described flow field for column and fracture flow experiments. Data for the measured and modelled experiments are taken from Table 4-1 and Table 5-1.*

| | Column measured | Column scoping | Fracture measured | Fracture scoping |
|---|---|---|---|---|
| Flow rate to channel | 6, 10 and 47.4 µl/min | 1 and 0.1 µl/min | 350 and 230 µl/min | 5 and 1 µl/min |
| Cv (transport to hydraulic aperture ratio) | 1.5 | 1.5 | 5.6 | 5.6 |
| Channel width | 4.4 cm | 4.4 cm | 20 cm | 20 cm |
| Channel length | 74.5 cm | 74.5 cm | 70 cm | 70 cm |
| Channel volume (hydraulic) | 17 ml | 17 ml | 13.5 ml | 13.5 ml |
| Correlation length of the velocity variation | 0.75 cm | 0.75 cm | 0.9 cm | 0.9 cm |
| Rock porosity | 0.2% | 0.2% | 0.2% | 0.2% |
| Rock density | 2600 kg/m$^3$ | 2600 kg/m$^3$ | 2600 kg/m$^3$ | 2600 kg/m$^3$ |
| Rock pore diffusivity | $2.4\cdot10^{-11}$ m$^2$/s | $2.4\cdot10^{-11}$ m$^2$/s | $2.4\cdot10^{-11}$ m$^2$/s | $2.4\cdot10^{-11}$ m$^2$/s |
| Diffusivity in free water | $10^{-9}$ m$^2$/s | $10^{-9}$ m$^2$/s | $10^{-9}$ m$^2$/s | $10^{-9}$ m$^2$/s |
| Volume of tubing | 1.27 ml | 1.27 ml | not taken into account [1)] | not taken into account |

[1)] Estimated delay in tubings (23 min and 20 min) subtracted from the measured breakthrough curves.

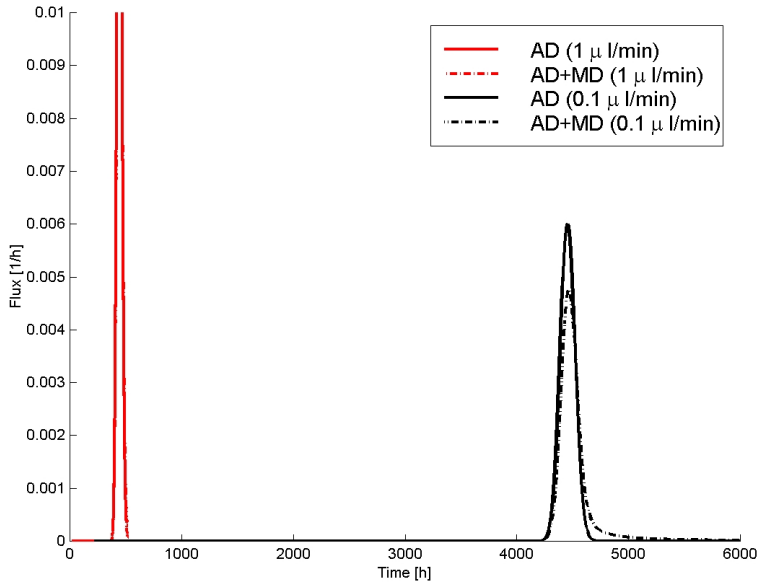


*Figure 7-1. Scoping calculations for the column experiment carried out with the cores of the boreholes. Applied parameters are presented in Table 7-1. Two flow rates that begin to show matrix diffusion, 1 μl/min and 0.1 μl/min, have been used in the calculations.*

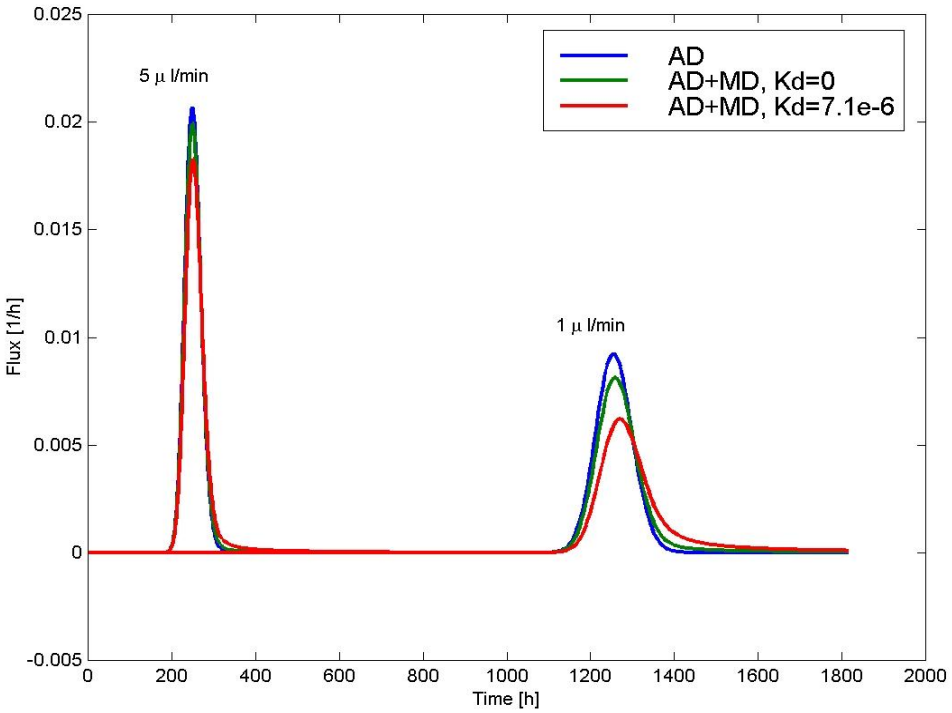


*Figure 7-2. Scoping calculation cases for a tracer test in fracture (from KR1 to side 3). Calculations are presented for two injection flow rates is 5 µl/min and 1 µl/min. It is assumed based on the previous tests that 25% of the flow goes to one channel. Other parameters are presented in Table 7-1. Results are presented for advection-dispersion (blue) AD and matrix diffusion of non-sorbing tracer (green) and AD and matrix diffusion of sorbing tracer ($K_d=7.1\cdot10^{-6}$ $m^3/kg$).*

# REFERENCES

**Hölttä, P. and Hakanen, M. 2002.** Fracture flow and transport experiments in laboratory scale: Testing experimental techniques and determining hydraulic characteristics using a large block. Posiva Oy, Working Report 2002-37.

**Hölttä, P., Poteri, A., Hakanen, M. and Hautojärvi, A., 2004.** Fracture flow and radionuclide transport in block scale laboratory experiments. Radiochim. Acta 92, 775-779 (2004).